Optimization of the design of SOFC systems with anode off-gas recirculation

V. Singh[a], I. Shukla[b], Z. Wuillemin[c], S. Diethelm[d] and J. Van Herle[e]

[a] *FUELMAT Group, EPFL, Switzerland, vaibhav.singh@epfl.ch*
[b] *FUELMAT Group, EPFL, Switzerland, isha.shukla@epfl.ch*
[c] *HTceramix, Switzerland, zacharie.wuillemin@htceramix.ch*
[d] *HTceramix & FUELMAT Group, EPFL, Switzerland, stefan.diethelm@epfl.ch*
[e] *FUELMAT Group, EPFL, Switzerland, jan.vanherle@epfl.ch*

Abstract:
In this work, we design and optimize a 3 kWe SOFC system with anode off-gas recirculation, for domestic heat and electricity demand in European households. Multi-objective criteria for the design optimization were the maximization of electrical efficiency and cogeneration efficiency. The system flowsheet which includes models for BOP components and an inhouse experimentally validated SOFC stack model, was solved using the software VALI.
For the design optimization, an initial population set with randomly assigned values of decision variables was created. The decision variables identified for the system were 1. Oxygen to carbon ratio before the external reformer 2. External to internal methane reforming fraction 3. Reducing fuel species molar fraction at anode outlet. Successive generations of population were computed by reproduction and mutation of the existing individuals. Following the 'survival of the fittest' rule, the iteration was stopped when a non-dominated solution set represented by a Pareto-optimal front was obtained.The results suggest that electrical efficiency upto 62.8 % and cogeneration efficiency upto 86.8 % could be reached.

Keywords:
SOFC system, electrical and cogeneration efficiency, decision variables, multi-objective optimization

1. Introduction

Small scale power generation (<10 kWe) using intermediate temperature solid oxide fuel cells has attracted widespread interest, due to the highest achievable electrical efficiencies amongst any technologies available [1].

To date, Ceramic Fuel Cells Limited's SOFC system 'Bluegen' holds the record for reaching net electrical efficiencies upto 60% [2]. Such SOFC systems use natural gas or biogas as fuel and consider steam methane reforming, with external steam supply, for syngas production and usage in the stack [3], [4]. Of particular relevance here, is a next generation system with anode exhaust gas recirculation [5], where a high overall fuel utilization can be achieved at low diffusion losses, leading to an improvement in the efficiency of the system. Further, since the recirculating feed contains steam produced in the stack, no external steam supply is needed for reforming. This eliminates the use of expensive water de-ionisation sets.

'HoTbox™' of HTceramix-SOFCPOWER [6] is the stack used in our proposed system. Unused fuel in the stack is combusted in a burner to complete the energy balance of the system. Excess heat recovered from the system is used for domestic heating. An electrically driven blower drives the anode exhaust back to the steam reformer. The system model, its' dimensioning and optimisation is elaborated in the following sections.

2. Methodology for system design and optimisation

A fourfold approach to design the required system is adopted (see figure 1). Firstly, a process flowsheet with models of the individual components is developed. The flowsheet is solvable once the values of the design variables are specified. Using pinch analysis techniques, internal heat recovery within the system is maximized. Thereafter, performance of the system is evaluated with respect to the desired multi-objectives. Lastly, an iterative optimization procedure is followed, using evolutionary algorithms, where the entire range of design variables is scanned.

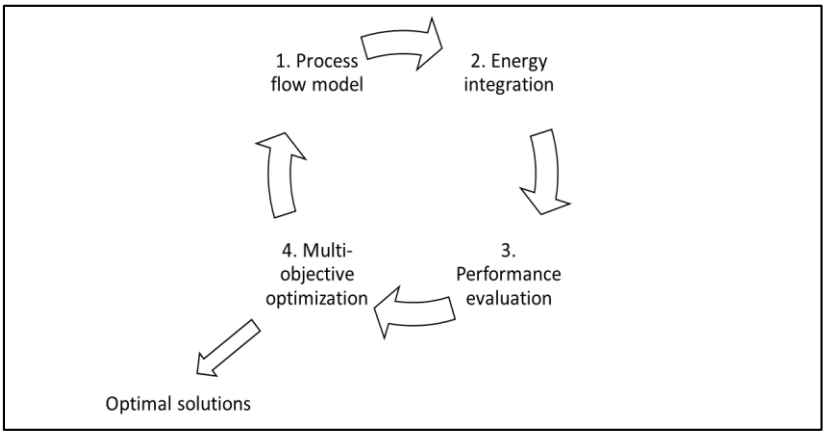

Figure 1. Methodology adopted for the system design

When the multi-objectives are conflicting, a non-dominated solution set represented by a Pareto-optimal front is obtained [7].

2.1. Process flow model

The system was modeled in the flowsheeting software VALI from Belsim S.A. Components of the system include a SOFC stack, heat exchangers, reformer, burner, recirculation blower, fan etc. The process schematic is shown in figure 2.

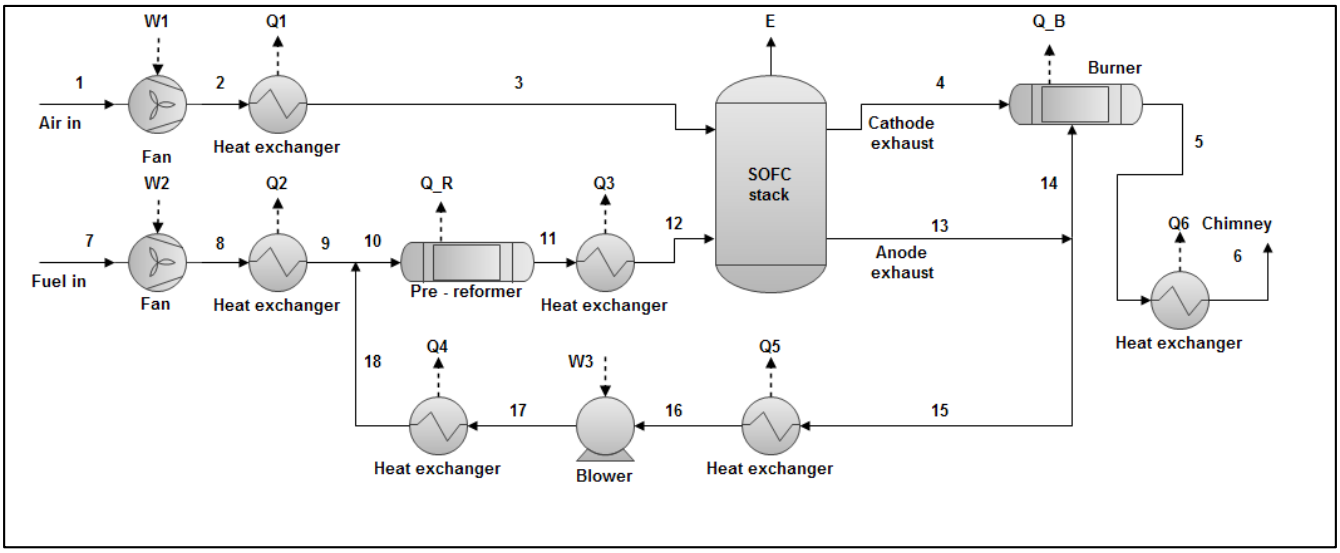

Figure 2. A schematic of the SOFC system

Methane (stream 7) and air (stream 1) are the feed gases to the system. The fuel is preheated to the reformer temperature (determined by external reforming fraction), where it mixes with the recirculating anode exhaust. Within the reformer, part of the methane is converted to hydrogen and carbon-monoxide. The reforming reaction is completed within the stack (internal reforming). Oxygen from the air feed is consumed in the electrochemical reaction at the cathode. The amount of fuel utilised in the stack is determined by the reducing fuel species fraction set at the anode exhaust. A fraction of the anode exhaust is sent to the burner, where it undergoes complete combustion, and provides the energy balance for the remaining processes in the system. The remaining fraction (determined by O/C ratio in the reformer) is recirculated back. Table 1 describes the design variables and their range of values. Details of the models on the individual components are presented next.

Table 1. Design variables and their range of variation

Design variables	**Range of values**
Oxygen to carbon ratio in reformer	2 to 3
Reducing fuel species fraction in anode exhaust (i.e. $CO+H_2$)	0.1 to 0.2
External reforming fraction	0.2 to 0.5

SOFC stack

The SOFC stack model used is an updated version of the one described in [8]. It has been validated with the performance maps of HoTbox™, the proprietary stack of HTceramix-SOFCPower. The stack receives the fuel supply (stream 12) in the anode compartment from the pre-reformer exit, and the incoming air (stream 3) in the cathode compartment, at an inlet temperature of 680°C. The amount of air intake (stream 1) is regulated such that an outlet stack temperature of 800°C is reached in a co-flow configuration. The following chemical reactions take place in the stack.

$CH_4 + H_2O \rightarrow CO + 3H_2$ *r×n1 (steam reforming)*

$CO + H_2O \rightarrow CO_2 + H_2$ *r×n2 (water gas shift reaction)*

$H_2 + 0.5O_2 \rightarrow H_2O$ *r×n3 (electrochemical reaction)*

The output stack voltage is calculated from the electrical power output (E) and stack current (I_{stack}).

Stack voltage, $V_{stack} = \frac{E}{I_{stack}}$ (1)

Voltage per cell, $V_{cell} = \frac{V_{stack}}{N_{cells}}$ (2)

Current density $j(A/cm^2) = \frac{I_{stack}}{A_{active}}$ (3)

Amount of oxygen consumed in the stack (Oxygen in stream 3 – Oxygen in stream 4)

$= \frac{I_{stack}.N_{cells}}{4F}$ (4)

Electrical power output of the stack is computed from the change in available Gibbs free enthalpy flow, and considering the irreversible losses. $E = (-\Delta \dot{G}_{stack}) - losses$ (5)

$\Delta \dot{G}_{stack} = (\dot{G}_4 + \dot{G}_{13} - \dot{G}_3 - \dot{G}_{12})$ (6)

$losses = I_{stack}^2.R_{ohmic} + (\eta_{anode,\ activation} + \eta_{cathodeactivation} + \eta_{anode,\ concentration} + \eta_{cathode,\ concentration}).N_{cells}.I_{stack}$ (7)

The irreversible losses are attributed to ohmic losses, activation losses and concentration losses.

Stack ohmic losses, $R_{ohmic} = \frac{R_{cell} \cdot N_{cells}}{A_{active}}$ (8)

Cell area specific resistance, $R_{cell}(\Omega cm^2) = R_{a,\,interconnect} + R_{c,\,interconnect} + fcc.R_{8YSZelectrolyte}$ (9)

where f_{CC} is a current collection factor, accounting for the electrode electrolyte interface.

Electrolyte conductance, $\sigma_{8YSZelectrolyte} = \sigma o_{8YSZelectrolyte} \cdot \exp\left(\frac{-E_{A,8YSZelectrolyte}}{RT}\right)$ (10)

The activation losses are calculated through the Butler Volmer equations:

$$j = j_{o,\,anode}\left[\exp(\frac{2F}{RT}\eta_{anode,\,activation}) - \exp(-\frac{F}{RT}\eta_{anode,\,activation})\right] \quad (11)$$

$$j = j_{o,\,cathode}\left[\exp(\frac{F}{2RT}\eta_{cathode,\,activation}) - \exp(-\frac{F}{2RT}\eta_{cathode,\,activation})\right] \quad (12)$$

$$j_{o,\,anode} = \frac{RT\sigma_{anode}}{3F}, \sigma_{anode} = \sigma_{o,\,anode} \cdot \exp\left(-\frac{E_{A,\,anode}}{RT}\right) \quad (13)$$

$$j_{o,\,cathode} = \frac{2RT\sigma_{cathode}}{F}, \sigma_{cathode} = \sigma_{o,\,anode} \cdot \exp\left(-\frac{E_{A,\,cathode}}{RT}\right) \quad (14)$$

Diffusion losses were modelled as described in [9], but are insignificant, as the stack operates significantly below the limiting current densities. Table 2 describes the values of parameters and operating variables used in the model.

Table 2. Used parameters in the model

Parameter description	**Used symbol**	**Value**
Electrical power output	E	3 kW
Active area of cell	A_{active}	80 cm2
Current density	j	0.4 A/cm^2
Stack inlet temperature	T_{in}	680 ºC
Stack outlet temperature	T_{out}	800 ºC
Recirculation temperature	T_r	200 ºC
Anode interconnect resistance	$R_{a,interconnect}$	0.02 Ωcm^2
Cathode interconnect resistance	$R_{c,interconnect}$	0.03 Ωcm^2
Current collection correction factor	fcc	4
Pre-exponential factor anode	$\sigma_{o,\,anode}$	433030 S/cm
Pre-exponential factor cathode	$\sigma_{o,\,cathode}$	4584515.9 S/cm
Pre-exponential factor electrolyte	$\sigma_{o,\,electrolyte}$	372.33 S/cm^2
Anode activation energy	$E_{A,anode}$	106000 J/mole
Cathode activation energy	$E_{A,cathode}$	101205 J/mole
Electrolyte activation energy	$E_{A,electrolyte}$	79535 J/mole
Electrolyte thickness	l_e	10 μm

Pre-reformer

The recirculating anode exhaust mixes with the incoming fuel supply just upstream of the reformer. The extent of external methane reforming or water gas shift reaction, considered at equilibrium, is determined by the operating temperature within the reformer.

$$CH_4 + H_2O \rightarrow CO + 3H_2 \qquad r \times n1$$

$$CO + H_2O \rightarrow CO_2 + H_2 \qquad r \times n2$$

Burner

In the burner, the unused fuel from the SOFC stack mixes with the cathodic exhaust and undergoes complete combustion in adiabatic conditions. The heat released in the process is either used for energy balance of the system or recovered. No pressure drop is considered in the burner.

$$CH_4 + 2O_2 \rightarrow CO_2 + 2H_2O \qquad r \times n4 \text{ (methane combustion)}$$

$$CO + 0.5O_2 \rightarrow CO_2 \qquad r \times n5 \text{ (CO combustion)}$$

$$H_2 + 0.5O_2 \rightarrow H_2O \qquad r \times n6 \text{ (hydrogen combustion)}$$

Heat Exchangers

Counter-flow heat exchangers are modeled. For system compactness and cost reductions, minimum approach temperatures in heat exchangers are restricted to the values mentioned in table 3.

Table 3. Constraints on minimum approach temperature

Stream	**Minimum approach temperature / 2 (ºC)**
Gas	25
liquid	15
Reformer stream	50
condensing stream	5

Recirculation blower and *fans*

An electrically driven blower circulates part of the anode exhaust back to the steam reformer. The fraction of recirculation is determined by the O/C ratio desired at the pre-reformer inlet. Due to its small size, isentropic efficiency of the blower is limited to 70%. The fans deliver the air and fuel supply to the system and consume minimal electrical power.

2.2. Energy integration

Excess heat produced in the system is recovered using water and used for domestic heating. The water undergoes heating from 20ºC to 60ºC. All the hot and cold streams in the system are shown in the composite curve (figure 3).

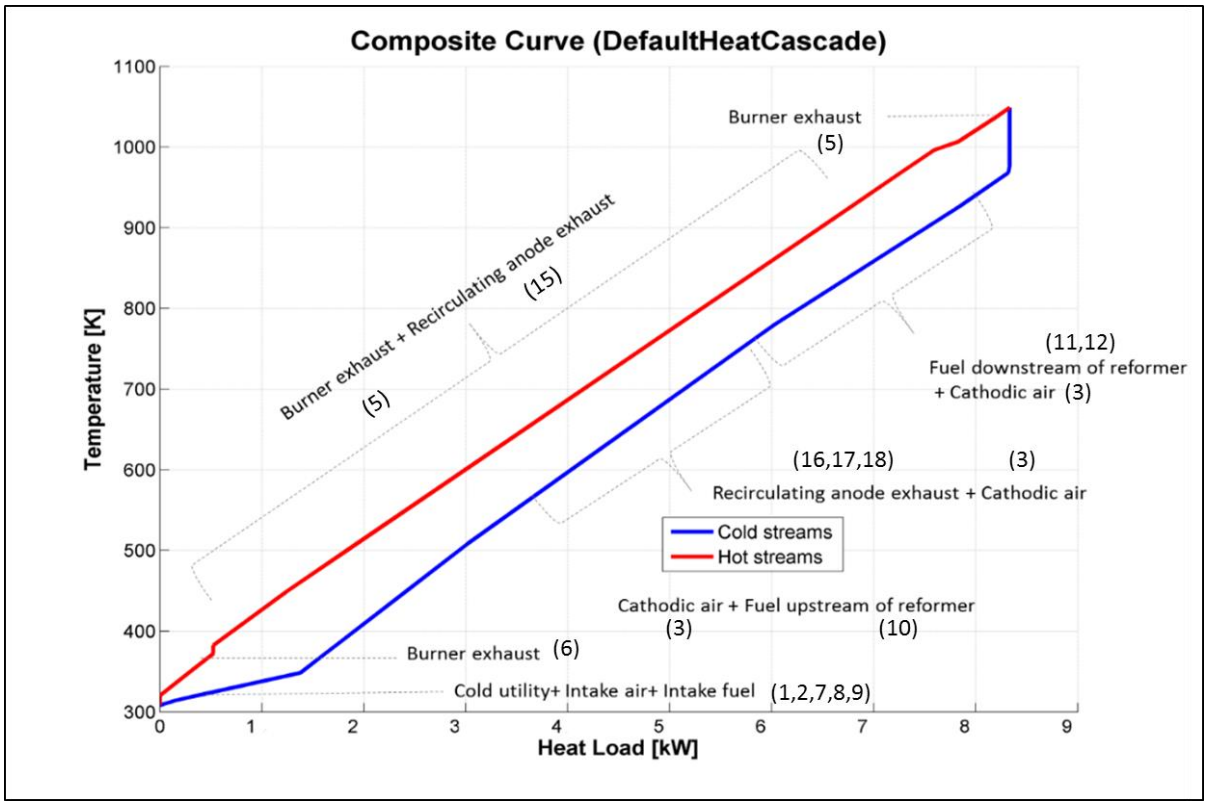

Figure 3. Composite curve showing the process and utility streams (numbers are the stream numbers as shown in figure 2).

There is no pinch point in the process. But for the simpicity of the system, there exists a greater potential of exergy recovery, than what is considered here.

2.3. Multi-objective optimisation

Evolutionary algorithms used for the optimization of energy systems have been described in [7]. Starting with an initial population of randomly assigned genes (i.e. the values of 3 decision variables), the flowsheet is solved for each individual. The members are evaluated based on the system electrical and cogeneration efficiency values.

where: Electrical efficiency $\eta_e = \dfrac{(E - W1 - W2 - W3)}{\dot{m}_7 \times LHV}$

Cogeneration efficiency $\eta_c = \dfrac{(E - W1 - W2 - W3) + \sum Q}{\dot{m}_7 \times LHV}$

W1, W2, W3 are the power consumption in the system (see figure 2).

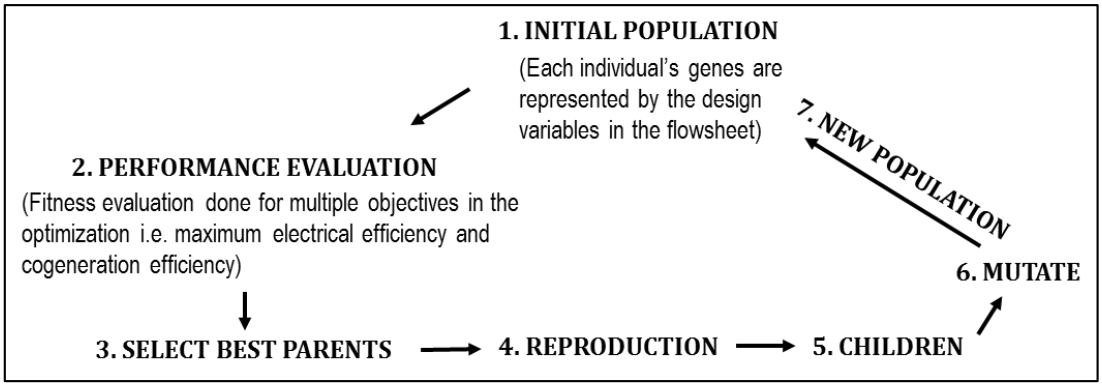

Figure 4. Steps involved in evolutionary algorithms

The worst performing individuals are discarded and the new population is generated by genetic crossover and mutations of the remaining individuals. The cycle (figure 4) is repeated till a non dominated solution set (represented by Pareto-optimal front) is obtained. The number of successive generations can be controlled in the algorithm.

3. Results and analysis

The iterative optimization is performed till a Pareto-optimal front is obtained. It is shown in figure 5.

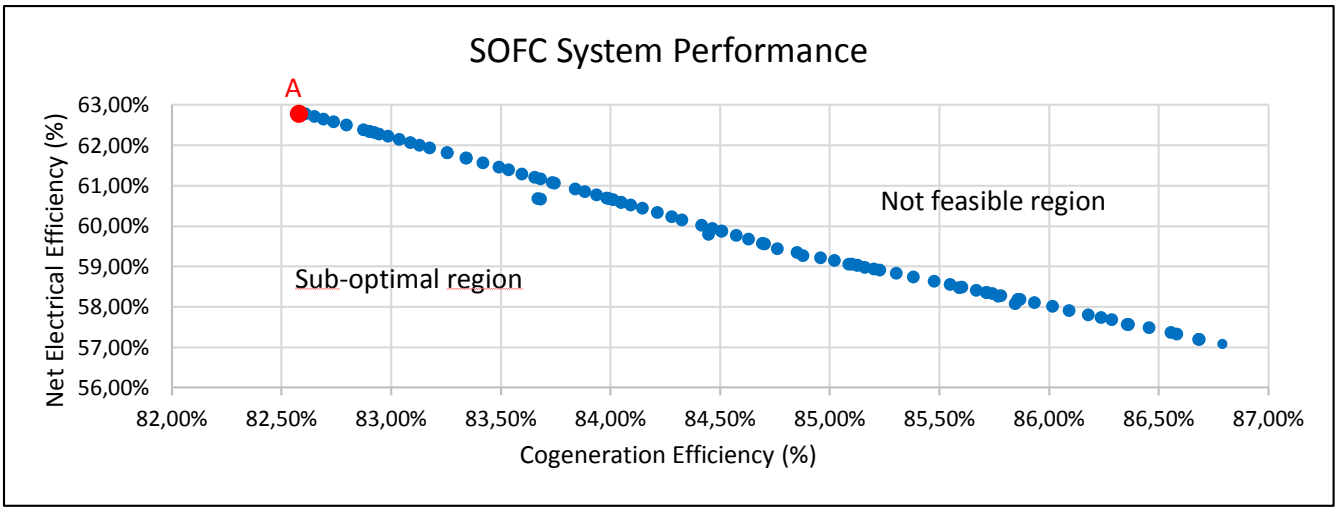

Figure 5. Optimized performance of the system

It is observed that for the chosen range of design variables, a maximum of 62.8 % electrical efficiency (stack DC – auxilliaries) and a cogeneration efficiency upto 86.8 % can be obtained. This is a commendable value and competes with the best in market on net electrical efficiency basis. The region above the Pareto is impossible to reach, due to irreversible losses in fuel cells, and some design constraints for system durability. Below the Pareto, the region is sub-optimal, as the points on the Pareto-optimal front showcase a better result with respect to the multiple objectives.

Figure 6 shows the evolution of design variables along the Pareto-optimal front. Two distinct kinds of solution sets are distinguished. The first kind corresponds to an O/C ratio of 2.7 at the reformer inlet, while the other corresponds to a value of 2. The same trend is observed in the reducing fuel species fraction, where there is a discontinuity at the border between two solution sets. A lower value of $CO+H_2$ fraction at the anode outlet, corrresponds to a higher electrical efficiency (more fuel consumption in stack) and lower cogeneration efficiency (less fuel burnt in burner).

External reforming fraction is restricted to the lower limit i.e. 20%. With more internal reforming, the amount of air feed to maintain the stack temperature gradient is lower, as some stack heat is taken away by the endothermic reaction. There is lower auxiliary power consumption in the fan, giving a better net electrical efficiency.

The trends in the other dependent variables (figures 7,8,9) are evident from the evolution of design variables. Since the total electric power output remains constant (i.e 3kWe), a lower single pass fuel utilization is compensated by higher recirculation (or higher O/C ratio at reformer), and vice versa. Global fuel utilization, which is a function of single pass fuel utilization and recirculation, varies accordingly.

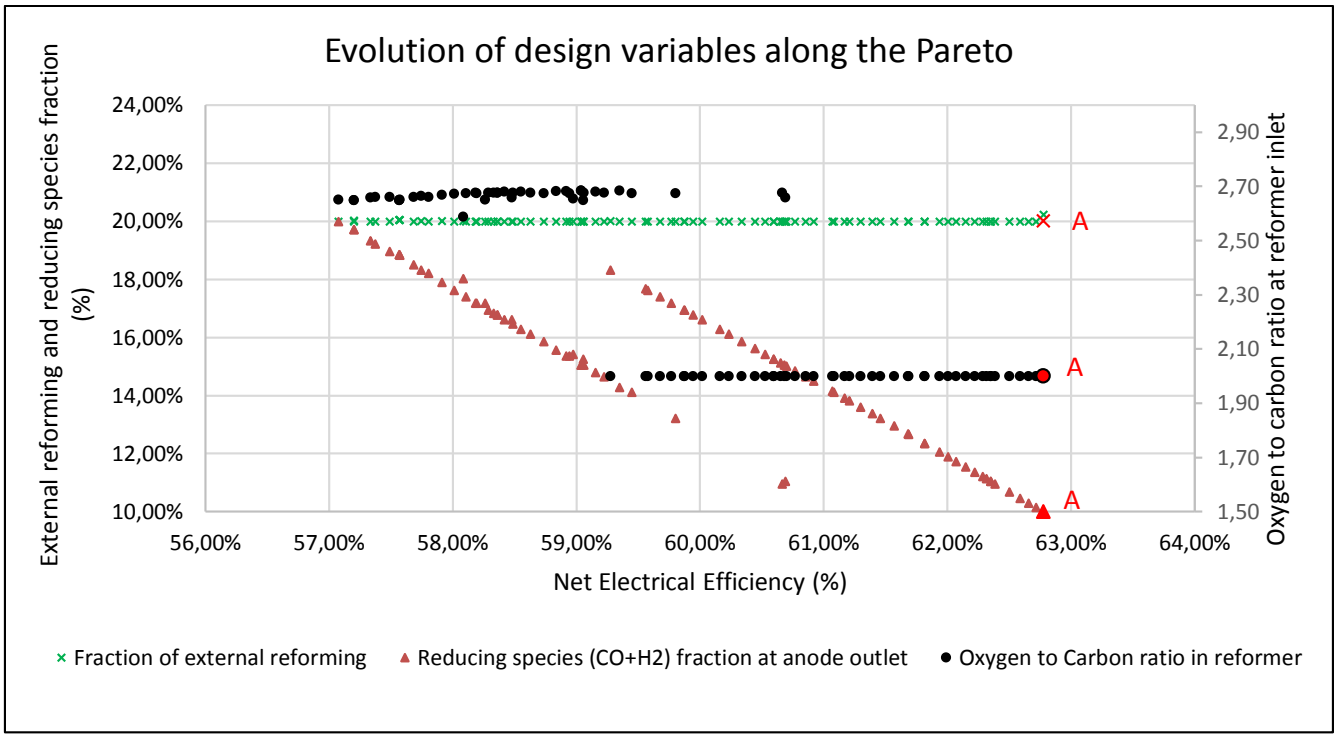

Figure 6. Evolution of design variables along Pareto front

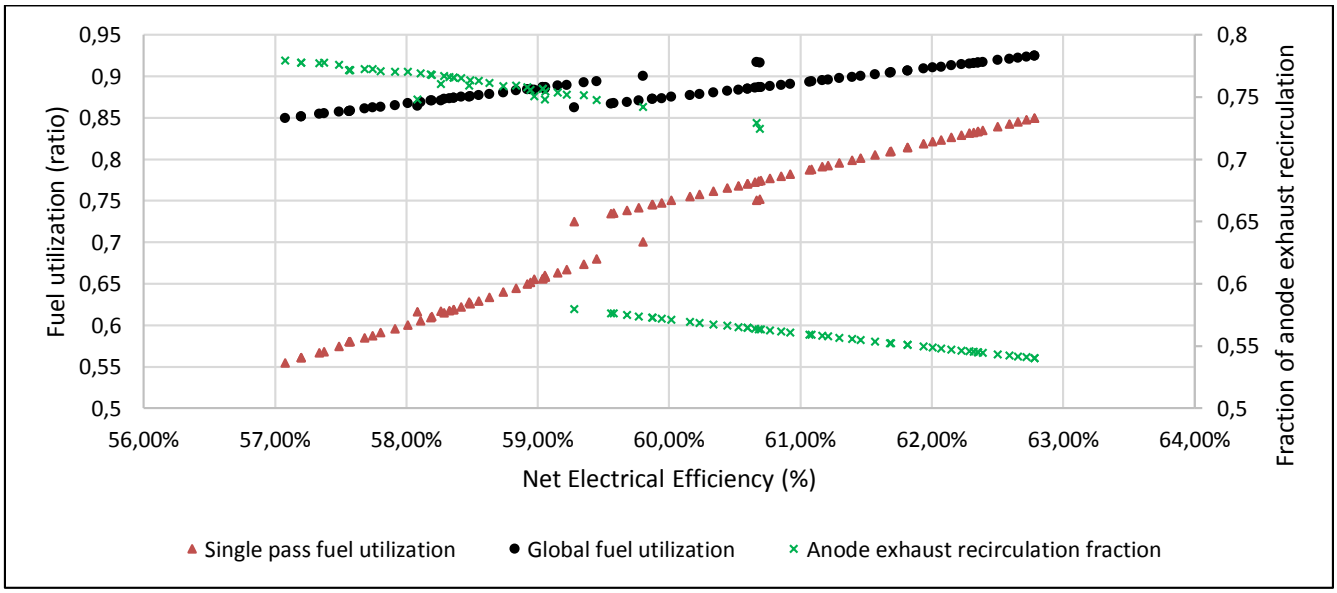

Figure 7. Evolution of fuel utilization, recirculation fraction along Pareto front

The cell voltage also shows a discontinuity for the two kinds of solution sets. It is higher for the case where single pass fuel utilization is higher and recirculation is less, as more hydrogen flows through the anode. The number of cells in the stack is inversely related to the cell voltage, with power and current being constant. Effectiveness of the most critical heat exchanger is less constrained (90% compared to 97%) at higher single pass fuel utilizations, as the air excess and thus heat capacity of cathode exhaust increases.

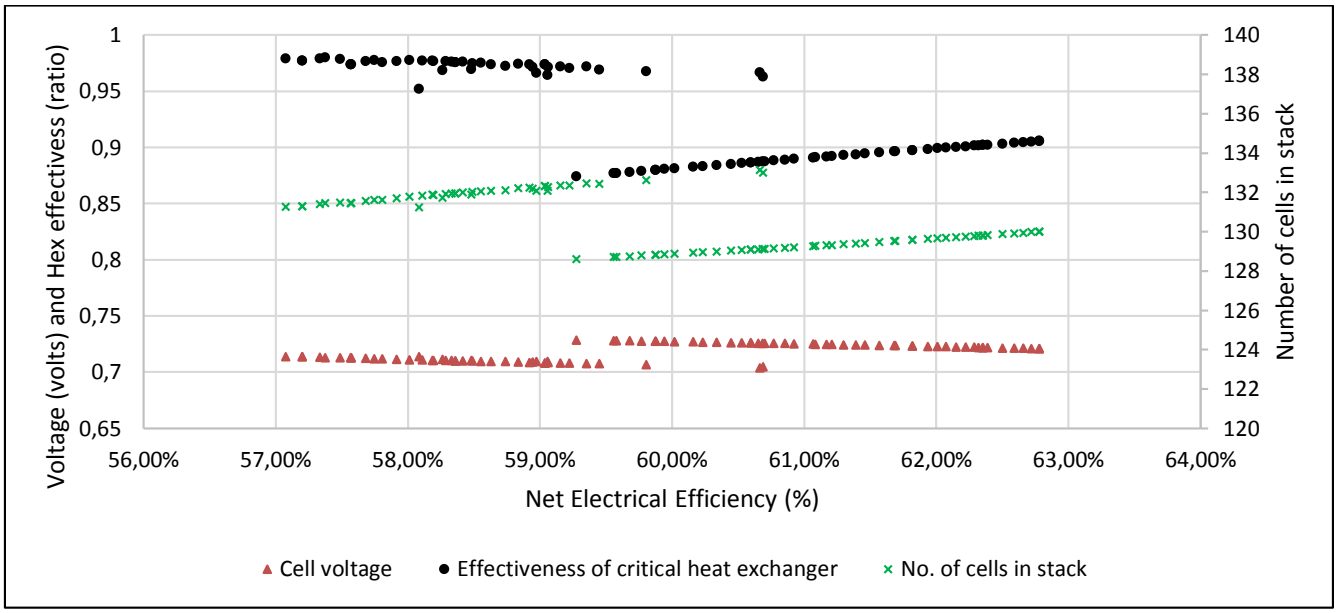

Figure 8. Evolution of cell voltage, no. of cells, heat exchanger effectiveness along Pareto front

For higher electrical efficiencies, more fuel is consumed in the stack and more heat produced. To maintain the stack temperature gradient of 120ºC, the cathodic air flow has to be increased. This also leaves less fuel to be combusted in burner, where the temperature decreases. The temperature in the reformer changes so as to maintain 20% external reforming, as the gas composition at its inlet varies with the change in recirculation percentage.

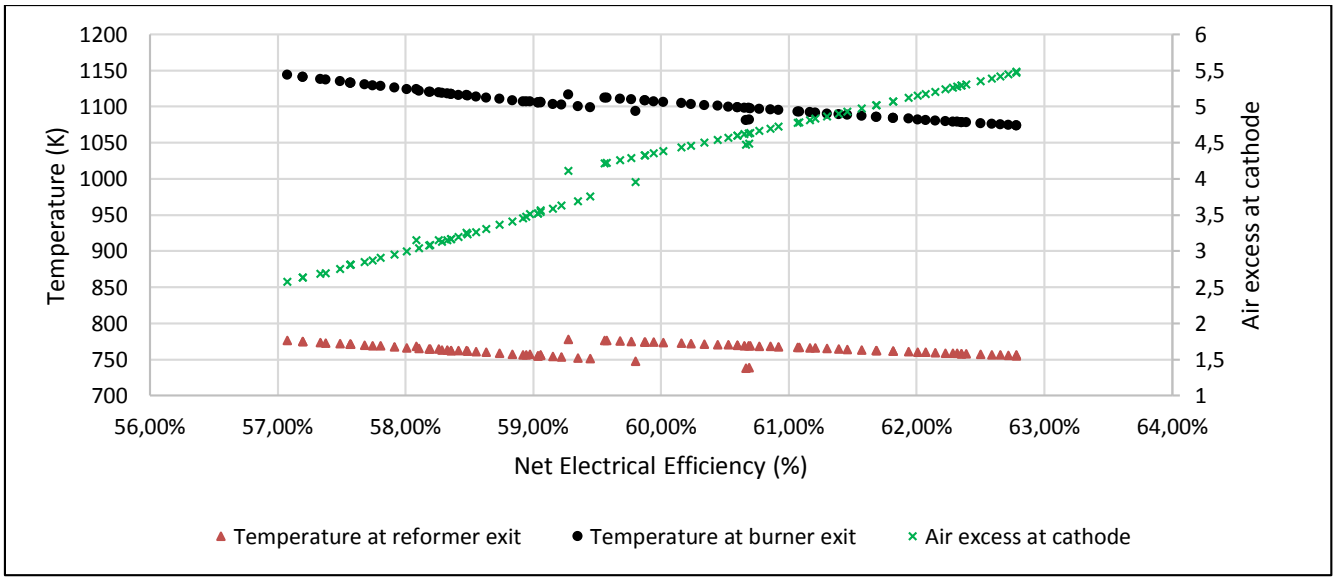

Figure 9. Evolution of temperature and air excess along Pareto front

For our proposed cogeneration system, we prioritise the maximisation of net electrical efficiency over cogeneration efficiency. Consequently, point A (see figures 5,6) is chosen as the design point. The values of the essential design and dependent variables at the operating point are summarised in table 4.

Table 4. Operating characteristics of the system at point A

System variable	**Operating value**
O/C ratio at reformer inlet	2.0
Reducing species fraction at anode exhaust	10 %
External reforming fraction	20 %
Mass flow rate methane (at 20ºC)	5.61 g/min
Air excess	5.47
Anode exhaust recirculation fraction	54 %
Reformer exhaust temperature	482 ºC
No. of cells in stack	130
Cell voltage	0.72 volts
Single pass fuel utilization	85 %
Global fuel utilization	93 %
Net electrical efficiency	62.8 %
Cogeneration efficiency	82.6 %
Pressure drop in SOFC stack	20 mbar
Power consumption in recirculator	7.86 W
Critical heat exchanger effectiveness	90.5 %
Heat exchanged Q_R	-324.95 W
Heat exchanged Q3	-254.27 W
Heat exchanged Q5	501.00 W
Heat exchanged Q4	-347.93 W
Heat exchanged Q1	-6705.0 W
Heat exchanged Q_B + Q6	8158.1 W
Heat exchanged Q2	0.00 W

4. Conclusion

Using a validated stack model, and simplified models of other BOP components, it is shown that the operation of SOFC systems can be optimized using evolutionary algorithms. There are two operation modes identified, i.e., 1. higher single pass fuel utilization and lower recirculation, and 2. lower single pass fuel utilization and higher recirculation. Electrical efficiencies in excess of 60% can be achieved.
In future, minimization of system costs will be included in the multi-objective optimization, for designing more market oriented systems. A more comprehensive model for the stack will replace the current zero-dimensional stack model created in Belsim VALI. This will however compete with the computational complexity involved in evolutionary algorithms. Further, a transient fuel cell model, incorporating degradation mechanisms, could aid in dynamic operation strategy to maximise durability and long term performance.

Acknowledgements

The authors would like to acknowledge the support of Siu Fai and Mardit Matian from HTceramix, and Priscilla Caliandro, Patrick Wagner, Arata Nakajo and Juerg Schiffmann from EPFL in aiding the work. This work would not have been possible without the software license from Belsim S.A., and the research grant from Canton deVaud under the '100 million de francs pour les énergies renouvelables et l'efficacité ènergétique'.

References

[1] E. Facchinetti, "Integrated solid oxide fuel cell - gas turbine hybris systems with or without CO2 separation," PhD thesis, EPFL, Lausanne, 2012.
[2] R. Payne, J. Love, and M. Kah, "CFCL's BlueGen product," presented at the ECS Transactions, 2011, vol. 35, pp. 81–85.
[3] Y. Shiratori, T. Ijichi, T. Oshima, and K. Sasaki, "Internal reforming SOFC running on biogas," *Int. J. Hydrog. Energy*, vol. 35, no. 15, pp. 7905–7912, 2010.
[4] S. Farhad, F. Hamdullahpur, and Y. Yoo, "Performance evaluation of different configurations of biogas-fuelled SOFC micro-CHP systems for residential applications," *Int. J. Hydrog. Energy*, vol. 35, no. 8, pp. 3758–3768, 2010.
[5] R. Peters, R. Deja, L. Blum, J. Pennanen, J. Kiviaho, and T. Hakala, "Analysis of solid oxide fuel cell system concepts with anode recycling," *Int. J. Hydrog. Energy*, vol. 38, no. 16, pp. 6809–6820, 2013.
[6] S. Modena, S. Ceschini, A. Contino, R. Bini, L. Tognana, M. Bertoldi, and Z. Wuillemin, "Evolution of SOFCpower' stack performances," presented at the ECS Transactions, 2013, vol. 57, pp. 359–366.
[7] G. Leyland, "Multi-objective optimisation applied to industrial energy problems," PhD thesis, EPFL, Lausanne, 2010.
[8] J. Van Herle, F. Maréchal, S. Leuenberger, and D. Favrat, "Energy balance model of a SOFC cogenerator operated with biogas," *J. Power Sources*, vol. 118, no. 1–2, pp. 375–383, 2003.
[9] Z. Wuillemin, "Experimental and modeling investigations on local performance and local degradation in solid oxide fuel cells," PhD thesis, EPFL, Lausanne, 2009.